PHYSICAL REVIEW E **83**, 056328 (2011)

Gas flow near a smooth plate

Adam P. Bowles and William A. Ducker*
Department of Chemical Engineering, Virginia Tech University, Blacksburg, Virginia 24061, USA

(Received 26 January 2011; revised manuscript received 21 April 2011; published 31 May 2011)

We examine gas flow adjacent to a molecularly smooth, solid, muscovite mica. The fluctuations in force acting on a glass sphere as a function of proximity to a mica plate were measured in air and were used to obtain the damping. The damping was interpreted as a lubrication force. The measured damping as a function of separation in the slip-flow regime corresponds to a slip length of 480 ± 70 nm, which is equivalent to highly specular gas molecule collisions. A slip-flow model fits the data for separations as small as one mean free path.

DOI: 10.1103/PhysRevE.83.056328 PACS number(s): 47.15.Rq, 47.45.Gx, 47.61.−k

I. INTRODUCTION

Recent research on gas flow in confined spaces confirms that boundary slip occurs at the solid-gas interface and that the magnitude of slip depends on the nature of the interface [1–6]. There are reports of particularly large slip lengths adjacent to carbon nanotubes [5,6]. For example, slip lengths up to 70 μm have been reported for water in a nanotube [5]. The primary objective of this work is to improve the understanding of gas flow in confined spaces adjacent to a molecularly smooth planar wall. Specifically, we examine gas molecule interactions with muscovite mica by measuring the lubrication force on a small, spherical particle approaching a flat plate. Secondary goals include testing the Vinogradova solution to the Navier-Stokes equations for squeeze flow near dissimilar surfaces [7] and developing a basis for more informed design of hard drive air bearings, semipermeable membranes, and microfluidics or microelectrical mechanical systems (MEMS) [8–10] where confined gas flows occur. Comparison to nanotube research can shed light on the importance of the degree of confinement on gas flows. In the work presented here, the gas is confined between two essentially flat parallel plates, whereas in the nanotube experiments, the gas is confined within a cylinder.

The flow of gases is usually classified into different regimes using the Knudsen number, which is the ratio between the mean free path, λ, and the characteristic length of the system, L. For the slip-flow regime, $1000\lambda > L > 10\lambda$, the slip length b is defined by the equation [11]

$$v_y(0) = b\frac{\partial v_y}{\partial z}. \tag{1}$$

In Eq. (1), v_y is the fluid velocity tangential to the interface, z is a direction normal to an interface, and $v_y(0)$ is the fluid velocity at the surface, i.e., at $z = 0$ (see Fig. 1). The slip length is sometimes used as a fitting parameter for experiments not in the slip-flow regime, e.g., for $L \sim \lambda/100$ in nanotube experiments [5,6] and even in liquids, $L > 1000\lambda$ [1,12–14]. Variation in slip length arises from the fact that, during a collision with a solid surface, a gas molecule will transfer some of its tangential momentum to the solid. The gas-solid interaction is characterized by the tangential momentum accommodation coefficient, σ, where $\sigma = 1$ represents diffuse reflection (gas molecule tangential momentum not conserved, minimum slip length) and $\sigma = 0$ represents specular reflection (gas molecule tangential momentum conserved, infinite slip length). The relationship between slip length and accommodation coefficient is [15]

$$b = \lambda\left[\frac{2.01}{\sigma} - 0.73 - 0.16\sigma\right]. \tag{2}$$

Note that even diffuse reflectance should produce a slip length of about the mean free path.

The flow profile of a gas is difficult to measure experimentally when fluids are confined to nanometer scale gaps. The indirect method of accessing the solid-gas boundary condition used here is to measure the damping force acting on a particle immersed in a gas and compare that force to the theoretical force obtained for a specific boundary condition. In the present work, we use a cantilever to hold a glass sphere ($R \sim 10$ μm) near a plate (see Fig. 1). The damping force due to collisions of gas (ambient air) with the sphere is measured using the atomic force microscope (AFM) detection system described previously [1]. The advantages of examining a cantilever that is adjacent to a wall compared to a cantilever in bulk fluid are that (a) the damping force is much larger in a squeeze film and (b) a single-sphere–cantilever probe can be used to interrogate gas flow over a variety of interesting surfaces without the need to fabricate a cantilever or sphere from that material. Previous AFM experiments with glass plates have found boundary conditions near the limit of diffuse reflectance. Maali and Bhushan [2] measured a slip length $b = 118$ nm for a glass probe and glass plate; Honig *et al.* [1] measured $b = 125$ nm for a methylated glass probe or methylated glass plate.

Mica is an interesting substrate because it can be cleaved to produce clean, molecularly smooth and rigid surfaces. A freshly cleaved surface of mica should enable highly specular collisions of the gas with the solid, but this cleanliness is compromised in our experiments by subsequent exposure to air. Importantly, the AFM experiment allows variation of the Knudsen number so that the slip length is measured both in the slip-flow regime (i.e., where the concept of slip is defined) and at smaller length scales approaching the free molecular regime.

*Author to whom correspondence should be addressed: wducker@vt.edu

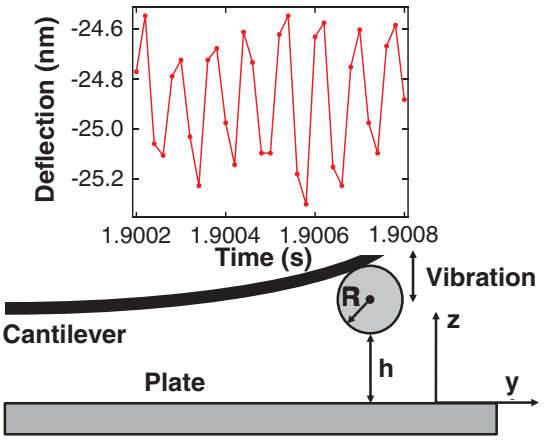

FIG. 1. (Color online) Schematic of a cantilever defining symbols used in the text. The inset shows a 0.6 ms sample of deflection fluctuations at a probe-plate separation of ∼1 μm in an experiment with $k = 0.067$ N/m and $R = 10.3$ μm.

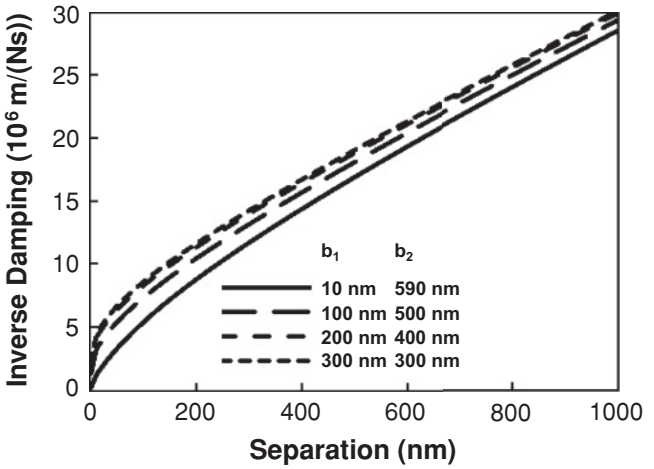

FIG. 2. Theoretical inverse damping for a combined slip length, $b_1 + b_2 = 600$ nm, calculated from the Vinogradova equation using $R = 11.9$ μm and $\eta = 1.86 \times 10^{-2}$ mPa s. The plot shows the effect of asymmetry, i.e., the effect of unequal slip length at the two surfaces. There is little difference between equal slip length and $b_1 = 200$ nm and $b_2 = 400$ nm, but there is a significant difference for large asymmetry, such as $b_1 = 10$ nm and $b_2 = 590$ nm. Comparing different combinations of b1 and b2, the slopes are similar in the slip-flow regime ($h > 500$ nm) but vary for $h < 200$ nm.

II. THEORY

A. Damped oscillator theory

The method of Honig *et al.* [1] is described briefly here. When a cantilever-sphere probe is immersed in a gas, the cantilever undergoes one-dimensional deflection fluctuations (see Fig. 1) with an average energy, $\frac{1}{2}k_B$T, which are mediated by collisions with the gas. We use the following equation for this motion [1]:

$$m\frac{d^2h}{dt^2} + D\,(h)\,\frac{dh}{dt} + kd = F_{\text{noise}} + F_{\text{surf}}\,(h)\,. \tag{3}$$

Here, m is the cantilever effective mass, t is time, D is the damping coefficient, k is the spring constant, d is the deflection of the cantilever, and h is defined in Fig. 1. F_{noise} is the force associated with the gas-mediated fluctuations. The influence of the plate is captured in two terms: $F_{\text{surf}}\,(h)$ which is a quasistatic surface force between the sphere and plate and $D(h)$, which we consider to be a combination of far-field damping $D(\infty)$ and the damping due to the proximity of the plate D_{lub}. We assume that m, $D(h)$, F_{surf}, and k are frequency independent. This is usually a good approximation when the damping and surface forces are small. Equation (3) can be rearranged to identify the energy spectrum density (ESD) near resonance as [1]

$$\frac{B}{\left[1-\left(\frac{f}{f_0(h)}\right)^2\right]^2 + \left(\frac{2\pi f\,D(h)}{k_{\text{eff}}(h)}\right)^2} + C, \tag{4}$$

where f is the frequency, f_0 is the resonant frequency, and k_{eff} is the effective spring constant under the influence of external forces. In Eq. (4), B, C, f_0, and $D(h)$ are adjustable parameters, which have distinct effects on the shape of the ESD. $D(h)$ controls the width of the spectrum. $D_{\text{lub}} = D(h) - D(\infty)$ is the contribution of the plate to the damping, which is then compared to a theoretical value to obtain b or σ.

B. Calculation of slip length

Vinogradova derived an equation for the lubrication damping force acting on a sphere driven towards a plate [7], which, via the fluctuation dissipation theorem, is the same as the damping observed in the ESD of the thermal fluctuations:

$$D_{\text{lub}} = \frac{6\pi\eta R^2}{h} f^*. \tag{5}$$

The fluid dynamic viscosity is given as η and R is the radius of the sphere. The slip lengths on the two solids, b_1 and b_2, enter into Eq. (5) via f^*:

$$f^* = -\frac{2\alpha h}{\beta\gamma} - \frac{2h}{\gamma-\beta}\left[\frac{(\beta+h)(\beta-\alpha)}{\beta^2}\ln\left(1+\frac{\beta}{h}\right) - \frac{(\gamma+h)(\gamma-\alpha)}{\gamma^2}\ln\left(1+\frac{\gamma}{h}\right)\right], \tag{6}$$

$$\alpha = b_1 + b_2, \qquad \beta = 2b_1(2+q+\sqrt{1+q+q^2}),$$
$$\gamma = 2b_1(2+q-\sqrt{1+q+q^2}), \qquad q = \frac{b_2}{b_1} - 1. \tag{7}$$

For $b_1 = b_2 = 0$, $f^* = 1$, recovering the result of Brenner [16]. In this work, we consider an asymmetric interaction [between glass coated with trimethylchlorosilane (TMCS) and mica]. It is important to note that for mild asymmetry ($|q|$ small), f^* is controlled by the sum of the slip lengths, $\alpha = b_1 + b_2$. This effect is shown in Fig. 2 for $b_1 + b_2 = 600$nm: D_{lub} is very similar for $b_1 = b_2 = 300$ nm and for $b_1 = 200$ nm, $b_2 = 400$ nm. When the lubrication force is sensitive only to the sum of the slip lengths, the effect of the probe cancels out for a series of measurements on different plates with the same probe.

III. EXPERIMENT

Mica (S&SJ, New York) for the plate was freshly cleaved immediately preceding an experiment. AFM images of these

surfaces over a 5 μm scan size indicate an rms roughness <0.1 nm. No steps were observed in a typical 5 μm scan. The fluctuation experiments used the D lever on an ORC8 chip (Veeco Metrology). Spring constants were determined by the Hutter method at $h > 1$ mm [17]. The three cantilevers employed here had $k = 0.067$, 0.070, and 0.062 N/m. A borosilicate glass probe (Duke Scientific) was attached to each cantilever with an epoxy (Epon Resin 1004F; Hexion Specialty Chemicals). Probe roughness was determined by inverse imaging with a TGT01 grating (NT-MDT). Probes with asperities greater than 10 nm above the apex of the sphere were rejected. The radii of the probes were measured using optical microscopy and were $R = 10.3$, 11.9, and 8.4 μm, respectively. Probes were coated with trimethylchlorosilane (99+% purity, Aldrich Chemical) to reduce the formation of water films on the surface, which make the system more difficult to model. The probes were irradiated for 90 min in a UV/Ozone ProCleaner (BioForce Nanosciences) and then placed in a vapor deposition chamber with 1–2 mL of TMCS overnight. The quality of the TMCS film was assessed by a contact angle study performed on a glass cover slip (FisherFinest Premium Cover Glass, thickness No. 1; Fisher Scientific) that underwent the same deposition procedure. Deionized water (Elix 3 followed by Synergy UV finishing; Millipore) was placed on the TMCS film in a FTA125 Contact Angle Analyzer (First Ten Angstroms). The contact angles were $95 \pm 3^\circ$ advancing, and $86 \pm 3^\circ$ receding. After removal, the probe again underwent inverse imaging and was rejected if it had been fouled.

Our AFM is an MFP-3D (Asylum Research) operating with closed-loop control on the piezo drive. The probe-plate contact area was exposed to atmospheric conditions (temperature: 21–24°C; humidity: 38–78 %). Experiments consisted of performing a 5–20 μm/s force curve to determine probe-plate separation. After returning (approximately) to its starting position, the probe dwelled for 10 s without controlled change of separation. Data were collected during this dwell at 50 kHz. A second force curve was then performed to identify any separation drift that occurred. This process was repeated in a series of increasing probe-plate separation steps to obtain the damping as a function of separation.

IV. RESULTS AND DISCUSSIONS

An example of the raw data is shown in Fig. 1 and the damping due to proximity to the plate, $D_{\rm lub}$, is shown in Fig. 3. $D_{\rm lub}$, as mentioned earlier, is obtained from the total damping, $D(h)$ by subtracting the damping at infinite separation [$D_{\rm lub} = D(h) - D(\infty)$]. $D(\infty)$ can be fitted from Eq. (4), evaluated at infinite separation, but in practice was derived from the quality factor, Q, in the Asylum thermal tune software using [1]

$$D(\infty) = \frac{k_\infty}{2\pi f_{0,\infty} Q_\infty}. \tag{8}$$

When h becomes large, the $D(\infty)$ correction becomes a significant fraction of the $D_{\rm lub}(h)$ signal. Therefore, a substantial error in $D(\infty)$ results in a considerable error in $D_{\rm lub}$. To minimize this effect we elect to only use data where $D(\infty) < 1/3D(h)$, which in practice corresponded to $h < 1000$ nm.

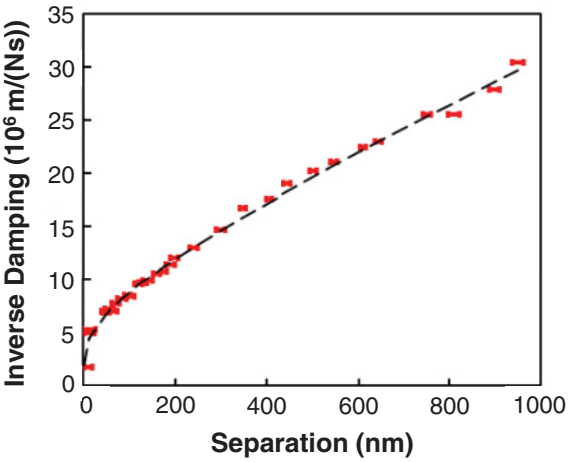

FIG. 3. (Color online) Measured inverse damping, $1/D_{\rm lub}$, by air squeezed between a mica plate and a TMCS-coated borosilicate glass sphere ($R = 11.9$ μm on a $k = 0.070$ N/m). The ends of the error bars in separation show separation at the beginning and end of the 10 s dwell period during each measurement. The dashed line represents the best fit to the data by the Vinogradova equation in the range 500–1000 nm (>7λ). The slip length on the mica was an adjustable parameter in this fit, which was 443 nm. Note that the fit to the Vinogradova equation also provides a good approximation to the data for $h <$ 200 nm.

Figure 3 shows that at large separation, $1/D_{\rm lub}$ is approximately linear, as expected. We fit Equation (5) to the data in the range 500−1000 nm, i.e. in the slip-flow regime ($h > 7\lambda$). For this fit we use the slip length of TMCS-coated glass established in literature ($b_1 \sim 125 \pm 50$ nm) [1]. The best fit returns a slip length on the mica of $b_2 = 443$ nm for the data shown in Fig. 3. The average over seven experiments gives $b_2 = 480 \pm 50$ nm for the mica plates. After including the error in b_1, the slip length on mica is $b_2 = 480 \pm 70$ nm.

From Fig. 3 one can see that the fit between the experimental data for separations in the range 500–1000 nm ($h > 7\lambda$) and the asymmetric Vinogradova solution is also excellent for separations approaching the order of a mean free path of air ($\lambda =$ 67 nm) [18]. In Fig. 4, the near contact region is examined for another plate-probe combination. For this $1/D_{\rm lub}(h)$ curve the parameters were fit to the data in the range 500–1000 nm with a $b_2 = 517$ nm. This fit is extrapolated to $h = 0.1$ nm. Excellent agreement is seen until $h \sim 100$ nm. Here, the gas is rarefied and continuum behavior (Navier-Stokes' equation) is not assured to adequately describe the confined gas flow, but in fact the theory and experiment agree quite well.

There are significant experimental difficulties in the region $h < 100$ nm, which are not included in the error bars shown, and prevent us from making a conclusion about the accuracy of the theory for small separations. Three experimental issues are noted here. First, the probe becomes overdamped near probe-plate contact making it difficult to ascertain the location and shape of the resonance peak. Second, the broadening of the resonance increases the range of frequencies examined. If any of the coefficients in Eq. (3) are functions of frequency in this range, then the solution [Eq. (4)] also has diminished accuracy.

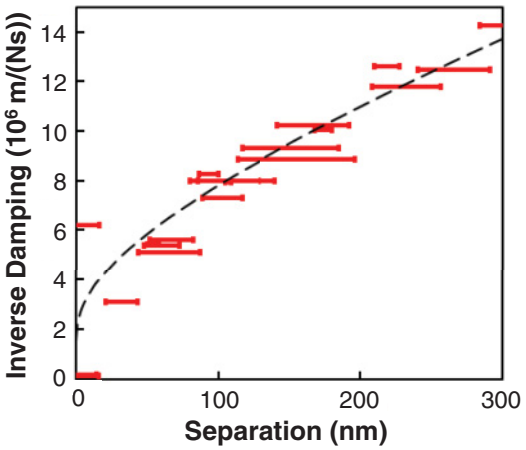

FIG. 4. (Color online) Near contact inverse damping coefficient for air squeezed between a TMCS-coated probe ($R = 8.4$ μm and $k = 0.062$ N/m). The dashed line is the Vinogradova solution that best fits the data ($b_2 = 517$ nm). The fit is in the range 500 nm $< h <$ 1000 nm (outside the bounds of this plot) and extrapolated to $h =$ 0.1 nm. Although unclear from this plot, $1/D_{\text{lub}}$ from the Vinogradova fit approaches zero as separation approaches zero. The figure shows good agreement between theory and experiment for $h >$ 100 nm.

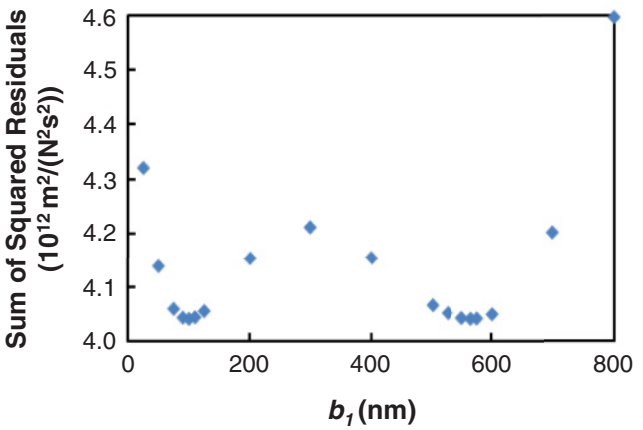

FIG. 5. (Color online) Sum of squared residuals between the experimental data and the Vinogradova fit as a function of fixed slip length on one plate. This plot demonstrates the ability of this technique to differentiate between the symmetric and asymmetric Vinogradova fits to the data. Minima are seen at $b_1 = 100$ nm and $b_1 \sim 550$ nm, showing the slip length of each surface.

Third, the variation of the inverse damping with respect to separation becomes larger at small h. We only monitor the separation at the beginning and end of the dwell and assume that it remains between these bounds during the dwell. This assumption becomes more critical at small separations where deviations in separation lead to large changes in damping. The most we can say is that the theory and experiment show roughly the same trend for $h <$ 100 nm.

For the experiments described here, the slip length of one the surfaces (TMCS-silica) was known in advance from the measurement of damping on a symmetric system, which left only one fitting parameter: the slip length on the plate. When the slip lengths on both surfaces are unknown, there are two cases. When the two slip lengths are similar, the damping is sensitive to the sum of the slip lengths, as described in Sec. II B, and various plates can be compared without needing to know the slip length on the probe. When the slip lengths are quite different, then the *shape* of the damping-distance curve depends on their relative magnitudes. This can be used to determine each of the slip lengths through a two-parameter (b_1,b_2) minimization of squared residuals between the experiment and Vinogradova theory. Figure 5 shows one slice through the two-parameter space for the data in Fig. 4, where at each point we fix b_1 and plot the minimum sum of squared residuals obtained when b_2 is allowed to vary. We see two distinct minima, at about 100 and 565 nm, showing that a single lubrication measurement on an asymmetric system can give slip lengths for the two surfaces simultaneously. These slip lengths are close to the values identified when we determined each individually: $b_1 = 125$ nm from an experiment where both surfaces had the same chemistry and $b_2 = 517$ nm using the asymmetric technique described in this work on this particular inverse damping curve.

The principal result of this work is that the slip length of air on mica is 480 ± 70 nm. This corresponds to $\sigma = 0.25 \pm 0.03$. This is consistent with predominantly specular reflections, as expected, since the mica surface is molecularly smooth and quite stiff. This result is not directly comparable to experiments measuring the flux through nanotubes because the latter are distinctly in the free molecular flow regime (1.2 nm $< h <$ 7 nm, $h < \lambda$), where the effects of confinement are very strong: our results bridge the gap between continuum and free molecular regimes but do show the effect of confinement to a lesser degree. We note that the slip lengths measured here for air are very similar to the slip length parameter that was previously obtained for *water in carbon nanotubes* by Holt *et al.*. ($\sim$400 nm) [6] and much smaller than the values for liquids fitted by Majumder *et al.*. (~ 10 μm) [5].

Comparison with the work of Maali and Bhushan as well as Honig and Ducker suggests that the boundary condition for lubrication in air is sensitive to changes in the surface. Maali and Bhushan found a slip length of 118 nm for glass surfaces with an rms roughness 1.2 nm and a peak-to-valley distance less than 4 nm [2]. The rougher plates produce greater accommodation of the gas, as expected. Honig and Ducker found that TMCS-coated glass has a slip length of 125 ± 50 nm [1]. The organic TMCS coating causes inelastic collisions allowing greater accommodation of the molecules. This is further corroborated by more recent work performed by Honig and Ducker [19] showing increasing slip length with decreasing amounts of organic material on the surface. Our earlier works give tangential momentum accommodation coefficients for comparable systems from other researchers [1,19].

This research has implications for situations in which the gas flows through small channels. For example, when a sphere with perfect accommodation (minimum slip boundary condition) approaches a flat plate with a slip length of 500 nm, the lubrication force at 500 nm separation is only 70% of the value that would occur if the slip length on the plate were 100 nm. (The minimum slip length in the slip-flow regime is approximately the mean free path of the

gas.) Similarly, the pressure drop in a capillary is affected by the boundary condition. For a gas in a cylinder (radius = 0.5 μm), solution of the Navier-Stokes equation [20] shows that the pressure drop is about three times smaller for a slip length of 500 nm as compared to that for a slip length of 100 nm.

The slip length scales with the mean free path which is, in turn, inversely proportional to P [15]:

$$b \propto \lambda \propto \frac{1}{P}. \tag{9}$$

Thus, the effect of the slip length extends further from the surface at lower pressures and thereby influences wider channels. For example, at $P = 0.01$ atm, the slip length on mica would be 50 μm.

V. CONCLUSION

The slip length on muscovite mica is large: $b = 480 \pm 70$ nm, as expected for a very smooth and stiff material. This slip length is much greater than for a rough material, and thus the properties of a solid surface can have a significant effect on the gas pressure drop across channels that are smaller than 1 μm when the pressure is less than or equal to 1 atm. There is quantitative agreement between the measured damping-separation data and the Vinogradova slip-flow solution. This agreement extends to the region when the gas is confined to a film that has a thickness that is similar to the mean free path of the gas. This ability to extend continuum force and flow models to molecular dimensions is seen elsewhere [10,21] and is useful for modeling. The experiment is sufficiently sensitive to distinguish between damping from asymmetric pairs of surfaces. Thus an experimenter could determine whether the sample and probe have different surfaces, if this were not already known.

ACKNOWLEDGMENTS

This work was funded by the National Science Foundation CBET-0828163. The authors acknowledge useful discussions with John Walz.

[1] C. D. F. Honig, J. E. Sader, P. Mulvaney, and W. A. Ducker, Phys. Rev. E **81**, 056305 (2010).
[2] A. Maali and B. Bhushan, Phys. Rev. E **78**, 027302 (2008).
[3] J. S. Jang and S. T. Wereley, J. Micromech. Microeng. **16**, 493 (2006).
[4] J. Maurer, P. Tabeling, P. Joseph, and H. Willaime, Phys. Fluids **15**, 2613 (2003).
[5] M. Majumder, N. Chopra, R. Andrews, and B. J. Hinds, Nature (London) **438**, 44 (2005).
[6] J. K. Holt, H. G. Park, Y. M. Wang, M. Stadermann, A. B. Artyukhin, C. P. Grigoropoulos, A. Noy, and O. Bakajin, Science **312**, 1034 (2006).
[7] O. I. Vinogradova, Langmuir **11**, 2213 (1995).
[8] Z. P. Duan and Y. S. Muzychka, Microfluid. Nanofluid. **3**, 473 (2007).
[9] P. Pandey and R. S. Chauhan, Prog. Polym. Sci. **26**, 853 (2001).
[10] N. Liu and D. B. Bogy, Tribol. Lett. **35**, 121 (2009).
[11] C. Neto, D. R. Evans, E. Bonaccurso, H.-J. Butt, and V. S. J. Craig, Rep. Prog. Phys. **68**, 2859 (2005).
[12] C. D. F. Honig and W. A. Ducker, J. Phys. Chem. C **111**, 16300 (2007).
[13] C. D. F. Honig and W. A. Ducker, Phys. Rev. Lett. **98**, 028305 (2007).
[14] C. D. F. Honig and W. A. Ducker, J. Phys. Chem. C **112**, 17324 (2008).
[15] C. R. Lilley and J. E. Sader, Proc. R. Soc. London, Ser. A **464**, 2015 (2008).
[16] H. Brenner, Chem. Eng. Sci. **16**, 242 (1961).
[17] J. L. Hutter and J. Bechhoefer, Rev. Sci. Instrum. **64**, 1868 (1993).
[18] G. A. Bird, *Molecular Gas Dynamics and the Direct Simulation of Gas Flows* (Oxford University Press, Oxford, 1996).
[19] C. D. F. Honig and W. A. Ducker, J. Phys. Chem. C **114**, 20114 (2010).
[20] R. B. Bird, W. E. Stewart, and E. N. Lightfoot, *Transport Phenomena*, 2nd ed. (Wiley, New York, 2002).
[21] A. P. Bowles, Y.-T. Hsia, P. M. Jones, J. W. Schneider and L. R. White, Langmuir **22**, 11436 (2006).